Available online at www.sciencedirect.com
ScienceDirect
Applied Surface Science 254 (2008) 4886–4890
applied surface science
www.elsevier.com/locate/apsusc

Oxygen flux influence on the morphological, structural and optical properties of $Zn_{1-x}Mg_xO$ thin films grown by plasma-assisted molecular beam epitaxy

S.C. Su [a,b], Y.M. Lu [a,c,*], Z.Z. Zhang [a], B.H. Li [a], D.Z. Shen [a], B. Yao [a], J.Y. Zhang [a], D.X. Zhao [a], X.W. Fan [a]

[a] *Key Laboratory of Excited State Processes, Changchun Institute of Optics, Fine Mechanics and Physics, Chinese Academy of Sciences, Changchun 130033, PR China*
[b] *Graduate School of the Chinese Academy of Sciences, Beijing 100049, PR China*
[c] *College of Materials Science and Engineering, Shenzhen University, Shenzhen 518060, PR China*

Received 14 November 2007; received in revised form 25 January 2008; accepted 26 January 2008
Available online 5 February 2008

Abstract

The $Zn_{1-x}Mg_xO$ thin films were grown on Al_2O_3 substrate with various O_2 flow rates by plasma-assisted molecular beam epitaxy (P-MBE). The growth conditions were optimized by the characterizations of morphology, structural and optical properties. The Mg content of the $Zn_{1-x}Mg_xO$ thin film increases monotonously with decreasing the oxygen flux. X-ray diffractometer (XRD) measurements show that all the thin films are preferred (0 0 2) orientated. By transmittance and absorption measurements, it was found that the band gap of the film decreases gradually with increasing oxygen flow rate. The surface morphology dependent on the oxygen flow rate was also studied by field emission scanning electron microscopy (FE-SEM). The surface roughness became significant with increasing oxygen flow rate, and the nanostructures were formed at the larger flow rate. The relationship between the morphology and the oxygen flow rate of $Zn_{1-x}Mg_xO$ films was discussed.
© 2008 Elsevier B.V. All rights reserved.

Keywords: $Zn_{1-x}Mg_xO$; P-MBE; Zn/Mg

1. Introduction

Recently, ZnO as a wide band-gap semiconductor with a large exciton binding energy of 60 meV [1], has attracted more and more attention for its potential applications in optoelectronic devices [2,3]. To realize ultraviolet (UV) light emitting diodes (LEDs) and lasers, one of key issues is the growth of heterojunctions and quantum wells for confining electrons and photons in the devices. Due to the similarity of the ionic radius between Mg^{2+} (0.57 A) and Zn^{2+} (0.60 A) [4], the wurtzite structure $Zn_{1-x}Mg_xO$ thin films were extensively studied as barrier materials for ZnO/ZnMgO quantum wells. Many groups have successfully reported the growth of single wurtzite phase $Zn_{1-x}Mg_xO$ layers [5–11], in which maximum Mg concentration is up to 49 at.%. We also have obtained the wurtzite structure $Zn_{1-x}Mg_xO$ thin film with Mg containing up to 30 at.% [12]. Most of these works were focused on the fabrication, structural and optical properties. However, there are few reports about the studies on the morphology controlling and growth mode for $Zn_{1-x}Mg_xO$ thin films until now, which were just important for obtaining the $Zn_{1-x}Mg_xO$ thin film with a smooth surface and two-dimensional (2D) growth for the fabrication of the quantum well structure. The influences of the growth parameters on the growing mode have been fully investigated in ZnO thin films. It is clearly that the II/VI ratio would strongly influence the interface morphology [13], surface morphology [14], and dislocation generation [15]. Then, it is essential to study the dependence of the oxygen flux on the crystal quality of the $Zn_{1-x}Mg_xO$ thin films. In these works, the composition control of the $Zn_{1-x}Mg_xO$ thin films were all to adjust the ratio of Zn/Mg. However, because Zn and Mg atoms are very active, a little varying of the source temperatures will cause larger change of Zn and Mg partial pressures. Therefore, it is difficult to control the composition by changing the metal source.

* Corresponding author: Tel.: +86 43186176322; fax: +86 43185682964.
E-mail address: ymlu@szu.edu.cn (Y.M. Lu).

0169-4332/$ – see front matter © 2008 Elsevier B.V. All rights reserved.
doi:10.1016/j.apsusc.2008.01.132

Table 1
The growth parameters and Mg contents of the $Zn_{1-x}Mg_xO$

Sample	Zn source T (°C)	Mg source T (°C)	Substrate temperature T (°C)	O_2 flow rate (sccm)	Growth pressure (mbar)	Mg content (x)
a	245	280	600	0.2	6×10^{-7}	0.20
b	245	280	600	0.4	8×10^{-7}	0.15
c	245	280	600	0.6	3×10^{-6}	0.06
d	245	280	600	0.8	1×10^{-5}	0.03

In this paper, $Zn_{1-x}Mg_xO$ thin films with single hexagonal phase were grown at a large range of the oxygen flux by P-MBE. The influences of oxygen flux on the structural, optical and morphological properties of the films were studied. By controlling the oxygen flow rate, two-dimensional (2D) growth of the $Zn_{1-x}Mg_xO$ thin films with the wurtzite structure was realized. The composition of $Zn_{1-x}Mg_xO$ thin films was controlled by adjusting the oxygen flow rate.

2. Experiments

The growth was carried out using a V80H molecular-beam epitaxy system equipped with Knudsen cells for a Zn solid source (99.9999%) and an Mg solid source (99.999%) as well as an radio frequency (rf)-plasma cell for oxygen source (O_2, 99.999%). The background vacuum of the growth chamber was about 1×10^{-9} mbar with supplying liquid nitrogen. A mass flux controller controls the oxygen flow rate. During the growth, the rf power of oxygen plasma was 300 W. The oxygen flow rate was varied 0.2–0.8 sccm, and the Zn source and Mg source were controlled at 245 °C and 280 °C, respectively. The *c*-plane sapphire (Al_2O_3) was used as the substrate. In order to obtain a clean fresh surface, the substrates were chemically etched in a hot solution of H_2SO_4:H_3PO_4 = 3:1 at 160 °C for 15 min. Before growth, the substrates were thermally pre-treated at 800 °C for 30 min, which was expected to remove surface contaminant and obtain oxygen terminated Al_2O_3 (0 0 0 1) surface. The films were grown at 600 °C.

X-ray diffraction (XRD) spectra were collected with a D/max–RA X-ray spectrometer (Rigaku International Corp., Japan) with Cu Kα radiation of 0.1543 nm to obtain the structural information of the films. A hatachi S4800 energy dispersive spectroscopy (EDS) was used to determine the Mg/Zn ratio in the films, and the acceleration voltage and the magnification of EDS were 10 kV and 5000, respectively. Optical transmission spectra were recorded using a Shimadzu UV-3101 PC scanning spectrophotometer. The sample morphology was investigated by a filed emission scanning electron microscope (SEM) (hatachi S4800). The photoluminescence (PL) measurements were performed on a JY-630 micro-Raman spectrometer. A He–Cd laser operating at 325 nm was used as the excitation.

3. Results and discussion

The Mg contents were detected by the EDS. The details growth parameters and Mg contents are given in Table 1. We obtained the $Zn_{1-x}Mg_xO$ films with different Mg contents through changing the oxygen flow rate and remaining the same of other conditions. The Mg content is decreased with the increasing the oxygen flow rate. The oxygen flow rates are 0.2, 0.4, 0.6 and 0.8 sccm corresponding to $Zn_{1-x}Mg_xO$ films with Mg contents x = 0.2, 0.15, 0.06 and 0.03, respectively. Because the Mg atom is more active than the Zn atom, the bonding between Mg and oxygen takes place more easily than that of Zn atoms. At low oxygen flow rate, the oxygen atom prefers binding with Mg atom to bonding with Zn, which results in the high Mg concentration in the $Zn_{1-x}Mg_xO$ films. As the oxygen flow rate increases, the Mg–O binding process saturates gradually, and more and more Zn atoms combine with oxygen atoms. In this case, the Mg content in the $Zn_{1-x}Mg_xO$ films is decreased. The EDS for the $Zn_{1-x}Mg_xO$ films are shown in Fig. 1. Only Zn, Mg, O and Al signals were detected in all the samples, indicating formation of the $Zn_{1-x}Mg_xO$ films with high purity. From EDS, it is found that all the $Zn_{1-x}Mg_xO$ films show metallic-rich characteristic.

Fig. 2 shows the SEM images of the surface of the $Zn_{1-x}Mg_xO$ layer grown under different oxygen flow rates. When the oxygen flow rate is 0.2 sccm, a flat surface morphology of $Zn_{1-x}Mg_xO$ film is obtained in Fig. 2(a). With increasing of the oxygen flow rate, the surface morphology of $Zn_{1-x}Mg_xO$ films becomes rough gradually. Many pits appear on the surface of the $Zn_{1-x}Mg_xO$ films at the oxygen flow rate of 0.4 sccm, as shown in Fig. 2(b). Fig. 2(c) and (d) exhibits that the nanostructures were formed on the surface of the $Zn_{1-x}Mg_xO$ films grown under higher oxygen flow rate conditions. The thicknesses of the grown films are measured by lateral image of SEM. The $Zn_{1-x}Mg_xO$ films thicknesses are 200, 250, 400, and 500 nm corresponding to the oxygen flow

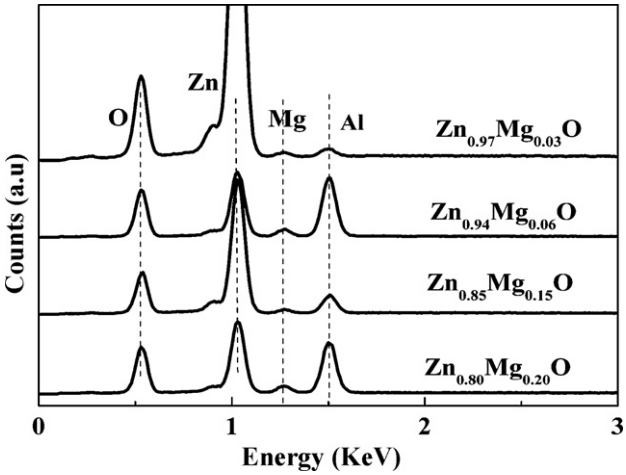

Fig. 1. The EDS of the $Zn_{1-x}Mg_xO$ films (x = 0.03, 0.06, 0.15, 0.20).

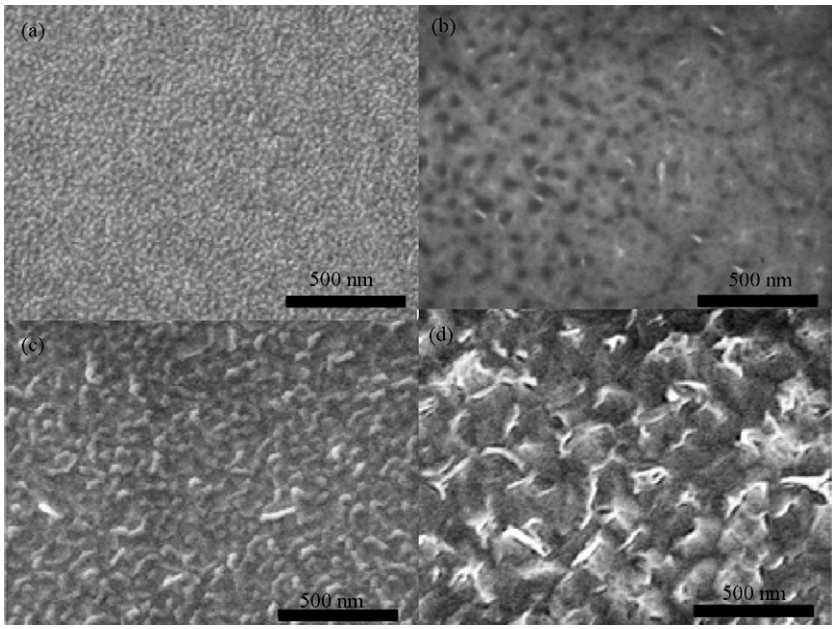

Fig. 2. SEM images from surfaces of the $Mg_xZn_{1-x}O$ layers grown at different oxygen flux: (a) 0.2 sccm; (b) 0.4 sccm; (c) 0.6 sccm; (d) 0.8 sccm.

rate are 0.2, 0.4, 0.6 and 0.8 sccm, respectively. The increase of the thickness with the increasing oxygen flow rate indicates that the growth rate is limited by the incorporation of oxygen atoms. It means that the $Zn_{1-x}Mg_xO$ thin films were grown under metallic-rich conditions. This is in good agreement with the result measured by EDS. In ZnO, it has been reported that the growth rate is restricted by the incorporation of Zn atoms under O-rich conditions. And the morphology structure of ZnO thin films with many pits was also observed in the Zn-rich conditions [16]. The possible reason of morphology evolution with increasing oxygen flow rate is that the activated oxygen atoms bind easily with the adsorbed metallic atoms. At low oxygen flow rate, the adsorbed metallic atoms could migrate to suitable lattice site through enough long distance due to the lack of oxygen. This leads to the growth of the $Zn_{1-x}Mg_xO$ thin films with 2D growing mode. In this case, the films growth velocity is slow and the surface looks smooth, as shown in Fig. 2(a). At the oxygen flow rate of 0.4 sccm, the absorbed metallic atoms, which did not fully migrate to suitable place, combine with the oxygen atoms to form $Zn_{1-x}Mg_xO$ thin films with many pits. As the oxygen flow rate increases further, the more and more metallic atoms bind with oxygen atoms as the nucleation site. In this case, the absorbed metallic atoms have not enough time to migrate, and the growth was carried out along a preferred direction. The growth velocity is increased and the nanostructures are formed on the surface of the $Zn_{1-x}Mg_xO$ films, as shown in Fig. 2(c) and (d).

Fig. 3 shows the XRD spectra for the $Zn_{1-x}Mg_xO$ films with different Mg contents of $x = 0.20$, 0.15, 0.06, 0.03 and 0, respectively. All the films have wurtzite structure with *c*-axis preferred orientation. No peak from other phases and impurities were observed. It should be noted that the diffraction peaks show asymmetrical line shape, which was caused by the superposition of diffractions from Kα1 and Kα2 lines. It indicates that the thin films have good crystal quality. With increasing oxygen flux, the position of the $Zn_{1-x}Mg_xO$ (0 0 2) peaks shifts from 34.68° ($x = 0.20$) to 34.44° ($x = 0$). This indicates that Mg^{2+} successfully replaces the Zn^{2+} in the ZnO lattice, and the Mg content is decreased with increasing of oxygen flow rate.

Fig. 4(a) gives the oxygen flow rate dependent on the Mg content in $Zn_{1-x}Mg_xO$. As the oxygen flow rate increases from 0.2 sccm to 0.8 sccm, the Mg content decreases from $x = 0.20$ to $x = 0.03$ in the $Zn_{1-x}Mg_xO$ films. The similar dependence of the lattice constant on Mg concentration is also observed in $Zn_{1-x}Mg_xO$ films. The *c*-axis lengths determined by XRD are plotted as a function of Mg contents in Fig. 4(b). When Mg content increases from $x = 0.03$ to $x = 0.20$, the *c*-axis lengths monotonically decreased from 5.203 Å to 5.168 Å.

To investigate optical properties of $Zn_{1-x}Mg_xO$ films, the room-temperature transmittance spectra were measured in the range of 200–800 nm, as shown in Fig. 5. The contribution of the Al_2O_3 substrate is excluded. These films are highly

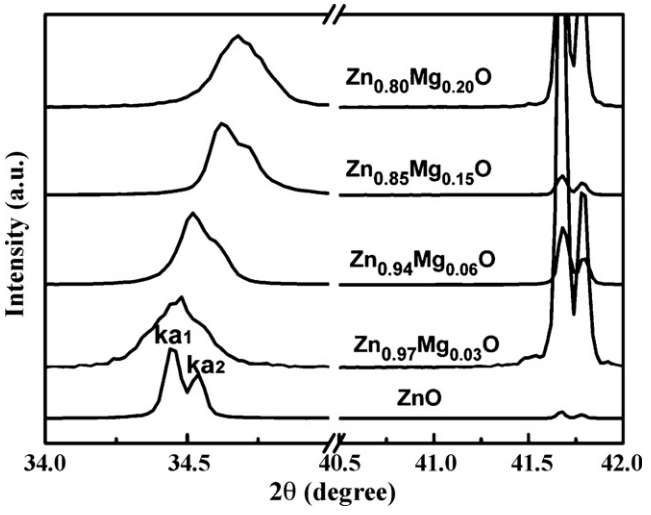

Fig. 3. The XRD spectra of the $Zn_{1-x}Mg_xO$ films with different Mg contents.

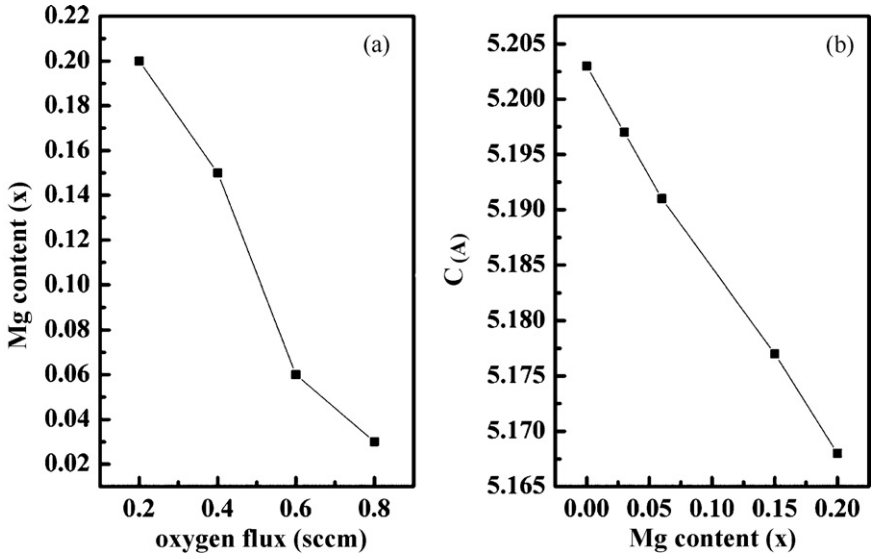

Fig. 4. Oxygen flux dependences of the Mg content in the $Zn_{1-x}Mg_xO$ films (a) and Mg content dependences of the *c*-axis lattice parameters in the $Zn_{1-x}Mg_xO$ films (b).

transparent in the visible region and have a sharp absorption edge in the UV region. The transmittances are about 80% in the visible region for all $Zn_{1-x}Mg_xO$ films. The absorption edge shifts to side of short wavelength as the Mg content increases. This shows clearly that the band-gap energy of $Zn_{1-x}Mg_xO$ alloy thin films depends on the Mg contents.

Since the interband transition in ZnO is the allowed direct transition, the optical-absorption coefficient α of ZnO can be derived using the following equation: $\alpha = (A/h\nu)(h\nu - E_g)^{1/2}$, where A is the proportional constant, $h\nu$ is the photon energy, and E_g is the optical band-gap energy. The E_g can be obtained by plotting $(\alpha h\nu)^2$ vs. $h\nu$ and extrapolating the linear portion to $\alpha = 0$. Using this method, the E_g of ZnO film is determined to be 3.29 eV with a steep absorption edge. In contrast, for the $Zn_{1-x}Mg_xO$ films, the E_g is, respectively, blue shifted from 3.32 eV ($x = 0.03$) to 3.67 eV ($x = 0.20$). The insert of Fig. 5 shows that the band-gap energy of films apparently varies linearly with the Mg content according to the relation E_g ($Zn_{1-x}Mg_xO$) = $2.1290x + 3.2858$ eV. The similar results are also obtained in other reports [17,18].

Fig. 6 shows room temperature photoluminescence spectra of the $Zn_{1-x}Mg_xO$ films with different Mg concentrations. The luminescence peak of the pure ZnO is observed at 3.29 eV, while the emission peaks of $Zn_{1-x}Mg_xO$ films show obvious blue-shifts with increasing Mg content. It is noted that the luminescence peak shifts to 3.66 eV at Mg concentration of 20%. The luminescence peaks of the $Zn_{1-x}Mg_xO$ films are broadened with increasing Mg content, which were also observed in other alloy semiconductors [19]. The origin of the strong emissions in the $Zn_{1-x}Mg_xO$ films will be reported elsewhere.

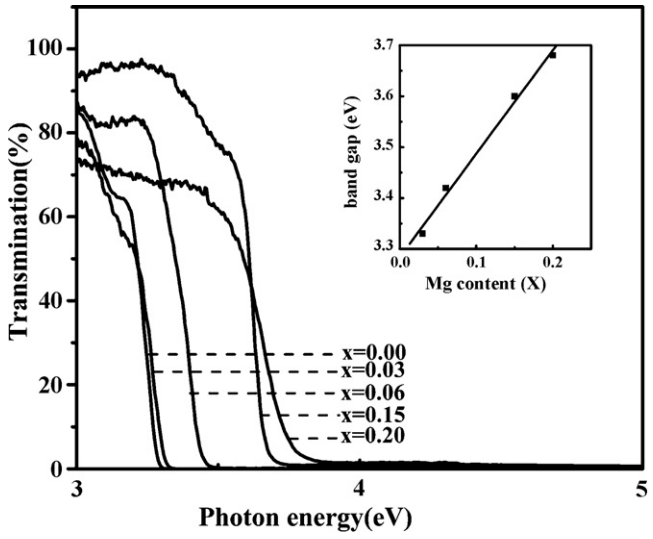

Fig. 5. Transmittance spectra of the $Zn_{1-x}Mg_xO$ films measured at room temperature. The insert shows the relationship between band-gap energy and Mg contents.

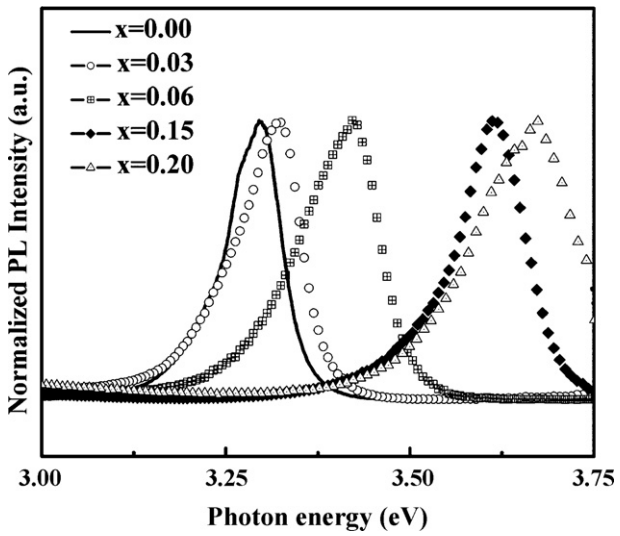

Fig. 6. The room temperature PL spectral of the $Mg_xZn_{1-x}O$ films with different Mg contents concentration grown on the Al_2O_3 substrate.

4. Conclusion

In summary, the single-phase $Zn_{1-x}Mg_xO$ films with *c*-axis oriented wurtzite structure were grown on Al_2O_3 substrate by P-MBE. It is feasible to adjust the Mg contents by changing the oxygen flow rate. With changing the oxygen flow rate from 0.2 sccm to 0.8 sccm, $Zn_{1-x}Mg_xO$ films with Mg contents of 0.2–0.03 were obtained. The morphology of $Zn_{1-x}Mg_xO$ films becomes roughness with the decreasing the oxygen flow rate. The 2D growing of the $Zn_{1-x}Mg_xO$ thin films with the wurtzite structure was obtained under low oxygen flow rates. This may be used as a method to realize precise control of growth parameters and alloy composition in the fabrication of the $Zn_{1-x}Mg_xO$ thin films.

Acknowledgments

This work is supported by the Key Project of National Natural Science Foundation of China under Grant No. 60336020, No. 50532050, the ‘‘973’’ program under Grant No. 2006CB604906, the Innovation Project of Chinese Academy of Sciences, the National Natural Science Foundation of China under Grant No. 60429403, No. 60506014, No. 50402016 and No. 10674133.

References

[1] K. Hummer, Phys. Status Solidi 56 (2000) 249.
[2] T. Soki, Y. Hatanaka, D.C. Look, Appl. Phys. Lett. 76 (2000) 3257.
[3] Z.K. Tang, G.K.L. Wong, P. Yu, Appl. Phys. Lett. 72 (1998) 3270.
[4] R.D. Shannon, Acta Crystallogr. Sect. A: Cryst. Phys. Diffr. Theor. Gen. Crystallogr. 32 (1976) 751.
[5] A. Ohotomo, M. Kawasaki, T. Koida, K. Masubuchi, H. Koinuma, Y. Sakurai, Y. Yoshida, T. Yasuda, Y. Segawa, Appl. Phys. Lett. 72 (1998) 2466.
[6] Y. Matsumoto, M. Murakami, Z. Jin, A. Ohotomo, M. Lippmaa, M. Kawasaki, H. Koinuma, Jpn. J. Appl. Phys. 38 (1999) 603.
[7] A.K. Sharma, J. Narayan, J.F. Muth, C.W. Teng, C. Jin, A. Kvit, R.M. Kolbas, O.W. Holland, Appl. Phys. Lett. 75 (1999) 3327.
[8] T. Minetomo, T. Negami, S. Nishikawa, H. Takakura, Y. Hamakawa, Thin Solid Films 372 (2000) 173.
[9] Y. Chen, H. Ko, S. Hong, T. Sekiguchi, T. Yao, Y. Segawa, J. Vac. Sci. Technol. B 18 (2000) 1514.
[10] W.I. Park, G. Yi, H.M. Jang, Appl. Phys. Lett. 79 (2001) 2022.
[11] S. Choopun, R.D. Vispute, W. Yang, R.P. Sharma, T. Venkatesan, H. Shen, Appl. Phys. Lett. 80 (2002) 1529.
[12] C.X. Wu, Y.M. Lu, D.Z. Shen, X.W. Fan, Chin. J. Semicond. 28 (2007) 701–704.
[13] S. Tomiya, H. Okuyama, A. Ishibashi, Appl. Surf. Sci. 243 (2000) 159–160.
[14] E.J. Tarsa, B. Heying, X.H. Wu, P. Fini, S.P. DenBaars, J.S. Speck, J. Appl. Phys. 82 (1997) 5472.
[15] B. Heying, R. Averbeck, L.F. Chen, E. Haus, H. Riechert, J.S. Speck, J. Appl. Phys. 88 (2000) 1855.
[16] Y. Chen, H.J. Ko, S.K. Hong, Y. Segawa, T. Yao, Appl. Phys. Lett. 80 (2002) 1358.
[17] S. Muthukumara, Y. Chen, J. Zhong, J. Cryst. Growth 261 (2004) 316–323.
[18] X.H. Wang, B. Yao, D.Z. Shen, Solid State Commun. 141 (2007) 600–604.
[19] K.P. O’Donnell, R.W. Martin, P.G. Middleton, Phys. Rev. Lett. 82 (1999) 237.